Thermochimica Acta, 138 (1989) 285–301
Elsevier Science Publishers B.V., Amsterdam – Printed in The Netherlands

THERMAL INVESTIGATION AND STEREOCHEMICAL STUDIES OF SOME CYCLIC DIAMINE COMPLEXES OF NICKEL(II), ZINC(II) AND CADMIUM(II) IN THE SOLID STATE. PART II.

LANGONJAM KANHAI SINGH and SAMIRAN MITRA *

Department of Chemistry, Manipur University, Canchipur, Imphal 795003 (India)

(Received 28 March 1988)

ABSTRACT

Acetato–cyclic diamine (piperazine (pipz), *N*-methylpiperazine (mpipz) and 1,4-diazacycloheptane (dach)) complexes of nickel(II), zinc(II) and cadmium(II) were synthesized. The thermal behaviour of these complexes was studied using thermogravimetry (TG) and differential thermal analysis (DTA) and the stereochemical changes occurring during thermal decomposition were investigated. The complexes were found to have the compositions $[Ni(pipz)(OAc)_2]\cdot 4H_2O$, $[Ni(mpipz)_2(OAc)_2]\cdot 2H_2O$, $[Ni(dach)_2](AcO)_2\cdot 2H_2O$, $[ML(OAc)_2]\cdot H_2O$ (M = Zn or Cd and L = pipz), $[Zn(mpipz)_2(OAc)_2]\cdot 2H_2O$, $[Zn(dach)(OAc)_2]\cdot H_2O$, $[Cd(mpipz)(OAc)_2]\cdot H_2O$ and $[Cd(dach)(OAc)_2]\cdot 0.5H_2O$. Attempts to prepare *N*,*N*′-dimethylpiperazine complexes failed. The characterization and study of configurational and conformational changes were carried out with the aid of elemental and thermal analyses, IR spectra and magnetic moment and conductivity measurements. The nickel complexes of pipz and mpipz, the zinc complex of mpipz and all the cadmium complexes appeared to be octahedral. The dach complex of nickel was square planar and the pipz and dach complexes of zinc were tetrahedral. The thermodynamic parameters, such as the activation energy E_a^*, the enthalpy change ΔH and the entropy change ΔS, for the dehydration steps and decomposition reactions of the complexes were evaluated using some standard methods. The order of stability of the complexes (with respect to E_a^*) follows the trend pipz > mpipz > dach. A linear correlation was found between E_a^* and ΔS for the decomposition reactions of the complexes.

INTRODUCTION

Although reports on acyclic diamine complexes are well known in the literature, research on cyclic diamine complexes, e.g. thermal investigations and stereochemical studies, is not as common [1–4]. We have attempted to synthesize some cyclic diamine (six- or seven-membered ring) complexes of transition and non-transition metals and to study their stereochemical changes during thermal decomposition. As a continuation of our previous

* Author to whom correspondence should be addressed.

0040-6031/89/$03.50

work [3,4], we report here the thermal investigation and stereochemical studies of acetato complexes of Ni^{II}, Zn^{II} and Cd^{II} with piperazine (pipz), *N*-methylpiperazine (mpipz) and 1,4-diazacycloheptane (dach) as cyclic diamine ligands.

On pyrolysis, these complexes first undergo dehydration followed by decomposition in single or multiple steps (Table 3). It is observed that before heating, the cyclic diamines in all the complexes function as bidentate chelating ligands (boat form). This is shown by the larger number of IR bands between 700 and 1400 cm^{-1} compared with those observed for the free ligand (chair form) [2–8]. The acetate ion in the complexes, in addition to its unidentate character and its existence as a counter anion in some complexes (Table 3), acts as a bidendate chelating and bridging ligand as shown by molar conductance and IR spectral data [9–17] (Table 2). In almost all of the complexes the $\nu_{as}(CO_2^-)$ bands are broad and strong. The broad nature of the $\nu_{as}(CO_2^-)$ bands also indicates the presence of more than one type of carboxylato group [17]. After heating under non-isothermal conditions these complexes undergo decomposition via intermediates (which cannot be isolated). In these intermediates the cyclic diamine may function as a bridging bidentate ligand (chair form) [2,6,18] so as to satisfy the coordination number of the metal ion and the acetate ion may act as a unidentate as well as a bridging bidentate agent.

Some thermodynamic parameters, such as $E_a^{\star}$, ΔH and ΔS for the dehydration and decomposition reactions of the complexes in the solid state are calculated. Some useful conclusions are drawn on the thermal stability of the complexes. The effects of *N*-alkylation of the ligand and ring size of the ligand on the stability of the complexes are considered.

EXPERIMENTAL

Materials and methods

Metal carbonates were of AnalaR grade and were used as received. Metal acetates were freshly prepared by neutralizing acetic acid with the corresponding metal carbonate and by subsequent slow evaporation. Piperazine obtained from Merck (F.R.G.) and *N*-methylpiperazine, *N*,*N*′-dimethylpiperazine and 1,4-diazacycloheptane (homopiperazine) obtained from Fluka AG (Switzerland) were used as received. Diethyl ether and ethanol were dried by standard procedures [19].

Preparation of the complexes

$[Ni(pipz)(OAc)_2] \cdot 4H_2O$

The ligand (ca. 0.516 g; 6 mmol) in dry ethanol (20 cm^3) was added with constant stirring to a solution of freshly prepared nickel acetate (ca. 0.746 g;

3 mmol) in dry ethanol (50 cm^3). The light blue nickel complex was collected by filtration, washed carefully with dry diethyl ether and dried over fused calcium chloride in a desiccator. Yield: 0.580 g, ca. 58%.

$[Ni(mpipz)_2(OAc)_2] \cdot 2H_2O$

A solution of freshly prepared nickel acetate (ca. 0.746 g, 3 mmol) in 50 cm^3 of dry ethanol was treated with the ligand (ca. 0.7 cm^3, 6 mmol) with constant stirring. An excess of dry diethyl ether was added and the mixture was kept overnight. Bluish crystals of the nickel complex were collected by filtration, washed with dry diethyl ether and dried over fused calcium chloride in a desiccator. Yield: 0.493 g, ca. 40%.

$[Ni(dach)_2](AcO)_2 \cdot 2H_2O$

The ligand (ca. 0.600 g, 6 mmol) in dry ethanol (20 cm^3) was added with constant stirring to a solution of the freshly prepared nickel acetate (ca. 0.746 g, 3 mmol) in dry ethanol (50 cm^3). An excess of dry diethyl ether was then added when a bright yellow precipitate of the nickel complex appeared. The complex was collected by filtration, washed carefully with dry diethyl ether and dried over fused calcium chloride in a desiccator. Yield: 0.870 g, ca. 70%.

$[ZnL(OAc)_2] \cdot H_2O$ (L = pipz or dach), $[Zn(mpipz)_2(OAc)_2] \cdot 2H_2O$

The ligand (ca. 4 mmol) in dry ethanol (20 cm^3) was added with constant stirring to a solution of freshly prepared zinc acetate (ca. 0.658 g, 3 mmol) in dry ethanol (30 cm^3) to give a white precipitate of the zinc complex, which was collected by filtration, washed with dry ether and dried over fused calcium chloride in a desiccator. Yield: ca. 60%.

$[CdL(OAc)_2] \cdot H_2O$ (L = pipz or mpipz)

Freshly prepared cadmium acetate (ca. 0.856 g, 3 mmol) in dry ethanol (30 cm^3) was treated with the ligand (ca. 4 mmol) in dry ethanol (20 cm^3) to form a white precipitate of the complex, which was collected by filtration, washed with dry diethyl ether and dried over fused calcium chloride in a desiccator. Yield: ca. 60–70%.

$[Cd(dach)(OAc)_2] \cdot 0.5H_2O$

The ligand (ca. 0.400 g, 4 mmol) in dry ethanol (20 cm^3) was added with vigorous stirring to a solution of freshly prepared cadmium acetate (0.856 g, ca. 3 mmol) in dry ethanol (30 cm^3). A sufficient quantity of dry diethyl ether was added to give a white precipitate of the complex, which was collected by filtration, washed with dry diethyl ether and dried over fused calcium chloride in a desiccator. Yield: 0.805 g, ca. 80%.

TABLE 1

Analytical (calculated values in parentheses) and magnetic data of piperazine (L), *N*-methylpiperazine (L′) and 1,4-diazacycloheptane (L″) complexes of Ni^{II}, Zn^{II} and Cd^{II}

Complex	Colour	Analysis (%)				μ_{eff} (BM)
		M	C	H	N	
1a $[NiL(OAc)_2]\cdot 4H_2O$	Light blue	17.02(17.54)	28.54(28.68)	7.06(7.17)	8.37 (8.38)	3.26
2a $[NiL'_2(OAc)_2]\cdot 2H_2O$	Bluish	13.80(14.22)	40.75(40.71)	8.80(8.24)	13.00(13.57)	3.20
3a $[NiL''_2](AcO)_2\cdot 2H_2O$	Yellow	13.69(14.22)	39.77(40.71)	8.88(8.24)	12.91(13.57)	
4a $[ZnL(OAc)_2]\cdot H_2O$	White	22.67(22.76)	33.11(33.40)	6.13(6.26)	9.32 (9.74)	
5a $[ZnL'_2(OAc)_2]\cdot 2H_2O$	White	15.53(15.59)	39.98(40.06)	8.09(8.11)	13.21(13.35)	
6a $[ZnL''(OAc)_2]\cdot H_2O$	White	21.22(21.70)	35.27(35.83)	6.57(6.64)	9.01 (9.29)	
7a $[CdL(OAc)_2]\cdot H_2O$	White	33.16(33.61)	28.62(28.71)	5.22(5.38)	8.17 (8.37)	
8a $[CdL'(OAc)_2]\cdot H_2O$	White	32.12(32.26)	30.80(31.00)	5.64(5.74)	7.98 (8.04)	
9a $[CdL''(OAc)_2]\cdot 0.5H_2O$	White	32.00(33.12)	32.78(31.82)	5.63(5.60)	8.37 (8.25)	

Elemental analysis, thermal study, IR spectra, magnetic moment and conductivity measurements

Nickel, zinc and cadmium were estimated gravimetrically using standard procedures [20]. Carbon, hydrogen and nitrogen were determined using Perkin–Elmer 240 C and Carlo Erba 1106 elemental analyzers. Results of elemental analyses are given in Table 1. Thermal investigations (TG and DTA) were carried out on a Shimadzu DT-30 thermal analyzer under a dynamic nitrogen atmosphere with a heating rate of 10 °C min^{-1}. α-Alumina was used as a standard. Indium metal was used as a calibrant for the evaluation of enthalpy changes. IR spectra were recorded with Beckman IR 20A and Perkin–Elmer 783 IR spectrometers using the KBr disc method. The effective magnetic moments were evaluated from magnetic susceptibility measurements using an EG and G PAR 155 vibrating-sample magnetometer at room temperature. Conductivity measurements of the complexes in DMSO at a concentration of 10^{-3} M were carried out at room temperature using a conductivity bridge (305 Systronics, India) and dip-type cell. Solid residues obtained after pyrolysis were identified by qualitative analysis [10].

RESULTS AND DISCUSSION

$[Ni(pipz)(OAc)_2] \cdot 4H_2O$ (1a)

This complex has been reported previously by Marcotrigiano et al. [14]. It has a light blue colour. Its lattice water is confirmed by the appearance of IR bands at 3300 and 3050 cm^{-1} (ν(OH)) and 1650 and 1560 cm^{-1} (δ(HOH)) (Table 2). Furthermore, the weight loss in the TG curve in the temperature range 60–119 °C and the endothermic peak in the DTA curve at 106 °C (Fig. 1) correspond to four molecules of lattice water (Table 3). The anhydrous complex $[Ni(pipz)(OAc)_2]$ (**1b**) is converted into $NiCO_3$ under non-isothermal conditions via the formation of $Ni(AcO)_2$. This process occurs in two steps, 1(b) and 1(c), in the ranges 155–286 and 286–380 °C, respectively. The corresponding DTA curve shows one exothermic peak at 282 °C for step 1(b) and another exothermic peak at 356 °C for step 1(c). The intermediate complex (**1b**) was not isolated.

The activation energy E_a^* can be evaluated from the TG curve using the equation of Horowitz and Metzger [21] and from the DTA curve using the equation of Borchardt and Daniels [22]. The values of E_a^* for the conversions **1a** → **1b**, **1b** → $Ni(AcO)_2$ and $Ni(AcO)_2$ → $NiCO_3$ from the TG and DTA * curves are 92.04 (114.80), 76.66 and 114.69 (169.86) kJ mol^{-1},

* Values of E_a^* from the DTA curves are given in parentheses.

TABLE 2

IR spectral data (cm^{-1}) for Ni^{II}, Zn^{II} and Cd^{II} cyclic diamine complexes

Complex	ν(NH) + ν(OH)	$\nu(CH_2)$	δ(NH) + δ(HOH) + $\nu_{as}(CO_2^-)$	$\delta(CH_2)$ + $\nu_s(CO_2^-)$	$\Delta\nu$	$\rho_\omega(CH_2)$	τ(NH) + ρ_ω(NH) + $\tau(CH_2)$	Stretching vibrations of skeleton ν(C–N) + ν(C–C)	$\rho_r(CH_2)$	$\delta(CO_2^-)$	ρ_r(NH) [a] + $\rho_r(CH_2)$ + ν(M–N)	ν(M–O)
1a $[NiL(OAc)_2]\cdot 4H_2O$	3300(sbr) 3050(sbr)	2980(w) 2890(w)	1700(br) 1650(w) 1580(sh) 1560(vsbr)	1450(sh) 1440(vs)	120	1390(sh) 1345(m)	1330(sh) 1260(w) 1150(sh) 1140(sh) 1120(m)	1100(w) 1070(vw) 1050(w) 1030(m) 1000(m)	960(vw) 940(vw) 905(sh) 890(s)	800(*mbr*)	660(s) 630(vw)	490(w) 400(w) 370(vw) 340(vw)
2a $[NiL'_2(OAc)_2]\cdot 2H_2O$	3420(br)	2950(vw) 2860(vw)	1700(vw) 1655(w) 1570(sbr) 1510(vw)	1460(vw) 1400(sh) 1390(vs)	180	1380(sh) 1360(sh)	1330(sh) 1150(vw)	1100(vw) 1075(vw) 1065(vw) 1045(vw) 1020(vw)	950(vw) 930(vw) 910(vw) 890(vw) 860(vw) 850(sh) 840(s)	825(sh) 820(sh) 810(vw) 780(vw) 730(w)	700(vw) 670(w) 660(w) 620(w) 550(vw) 500(vw)	460(vw) 425(vw) 400(vw)
3a $[NiL''_2](AcO)_2\cdot 2H_2O$	3460(br) 3130(vs) 3100(w)	2940(vw) 2900(vw) 2870(vw)	1650(wbr) 1570(sbr) 1550(sh)	1485(vw) 1475(ms) 1460(m) 1445(sh) 1430(s) 1420(s)	140 (150)	1385(w) 1370(m) 1345(w)	1325(sh) 1310(m) 1300(w) 1260(w) 1250(sh) 1230(vw) 1150(w) 1130(m)	1080(s) 1050(vw) 1020(vw) 990(s)	925(w) 890(vw) 855(m)	780(ms)	655(sh) 645(ms) 625(sh) 580(vw) 560(w) 540(vw)	
4a $[ZnL(OAc)_2]\cdot H_2O$	3380(sbr)	2930(vw) 2860(vw)	1650(w) 1570(sbr) 1510(m) 1500(sh)	1430(sh) 1390(s)	180	1350(w)	1300(vw) 1240(vw) 1220(vw) 1205(vw) 1150(vw)	1090(sh) 1050(w) 1020(vw) 1000(sh)	940(w) 880(w) 835(m)	800(sh) 740(w)	710(w) 680(w) 620(w) 520(vw)	470(w) 365(w) 310(sh)
5a $[ZnL'_2(OAc)_2]\cdot 2H_2O$	3380(br) 3200(br)	2950(w) 2910(m) 2830(vw)	1640(w) 1620(sh) 1590(sh)	1490(vw) 1430(sh) 1400(sbr)	150	1350(w)	1330(w) 1315(vw) 1305(sh)	1110(vw) 1085(m) 1040(w)	920(w) 890(w) 855(m)	765(w)	660(m) 630(vw) 610(w)	480(vw) 415(vw) 370(vw)

		2780(sh) 2760(w) 2750(sh) 2720(w)	1550(vsbr) 1505(sh)				1285(vw) 1275(w) 1265(vw) 1185(vw) 1165(w) 1130(m)	1025(m) 1015(vw) 1005(w) 985(m)	850(sh)		580(vw)	360(w) 315(vw)
6a $[ZnL''(OAc)_2]\cdot H_2O$	3420(br)	2920(w) 2850(w)	1620(w) 1560(sbr) 1540(m) 1505(m)	1490(w) 1460(vw) 1440(w) 1385(sbr)	175	1340(w)	1220(w) 1170(vw) 1160(vw) 1140(vw)	1070(vw) 1050(vw) 1020(vw)	950(vw) 935(vw) 925(vw) 915(vw) 900(vw) 890(w)	805(w) 770(vw) 750(vw) 720(sh)	680(w) 625(w) 605(w)	470(sbr) 400(s)
7a $[CdL(OAc)_2]\cdot H_2O$	3340(sbr) 3210(s)	2960(w) 2940(w) 2860(vw) 2840(vw)	1650(wbr) 1620(sh) 1570(sbr)	1450(m) 1425(s) 1410(sh)	145	1370(sh) 1340(vw)	1330(vw) 1325(vw) 1260(sh) 1255(m)	1090(s) 1060(vw) 1050(vw) 1020(s) 1005(vw) 1000(m) 995(m)	925(vw) 890(sh) 875(s)	825(vw) 800(vw)	670(vw) 645(w) 620(vw) 600(sh)	470(w) 365(w) 325(vw) 300(vw)
8a $[CdL'(OAc)_2]\cdot H_2O$	3410(sbr) 3235(w)	2980(w) 2940(w) 2860(w) 2815(vw) 2810(w)	1650(wbr) 1630(vw) 1560(sbr) 1540(w)	1455(w) 1440(m) 1430(s) 1410(m)	130	1360(vw) 1340(vw)	1300(m) 1290(s) 1280(m) 1200(s) 1185(s) 1180(vs) 1165(vw) 1145(vs) 1120(vw)	1100(vs) 1060(sh) 1050(m) 1040(s) 1030(m) 1020(s) 1000(vs) 995(sh)	935(m) 910(m) 870(vs) 835(vw)	800(sh) 780(s)	680(sh) 675(vs) 650(w) 630(m) 605(vw) 500(w)	485(vw) 430(w) 390(sh) 375(w)
9a $[CdL''(OAc)_2]\cdot 0.5H_2O$	3420(br) 3280(m) 3220(m)	2980(sh) 2940(m) 2880(vw)	1650(wbr) 1635(vw) 1560(sh) 1555(vsbr)	1470(w) 1440(sh) 1415(sbr)	140	1375(w) 1340(w)	1290(w) 1270(w) 1245(vw) 1210(w) 1145(m)	1105(w) 1070(w) 1045(w) 1030(w) 1020(w) 1010(m) 980(w)	930(w) 865(sh) 845(s)	810(vw) 780(vw) 770(vw) 760(vw) 745(vw)	670(m) 665(sh) 630(w) 605(vw) 535(w) 500(w)	480(vw) 460(vw) 435(vw) 370(w) 320(w)

Underlined frequencies are taken for the separation $\Delta\nu$ between $\nu_{as}(CO_2^-)$ and $\nu_s(CO_2^-)$. [a] Frequencies above 650 cm^{-1} may overlap with those of $\delta(CO_2^-)$. L = piperazine, L' = *N*-methylpiperazine, L'' = 1,4-diazacycloheptane. v = very, s = strong, m = medium, w = weak, br = broad and sh = shoulder.

TABLE 3

Thermal parameters of cyclic diamine [a] complexes of Ni^{II}, Zn^{II} and Cd^{II}

Decomposition reaction	Temperature range (°C)	DTA peak temperature (°C)		E_a^* (kJ mol^{-1})		Enthalpy change ΔH (kJ mol^{-1})	Entropy change ΔS (J K^{-1} mol^{-1})
		Endo	Exo	TG	DTA		
1a $[NiL(OAc)_2]\cdot 4H_2O \rightarrow [NiL(OAc)_2]$	60–119	106	–	92.04	114.80	190.22	501.90
1b $[NiL(OAc)_2] \rightarrow Ni(AcO)_2$	155–286	–	282	76.66	–	29.28	61.64
1c $Ni(AcO)_2 \rightarrow NiCO_3$	286–380	–	356	114.69	169.86	60.01	95.41
2a $[NiL'_2(OAc)_2]\cdot 2H_2O \rightarrow [NiL'_2(OAc)_2]$	80–215	125	–	21.27	–	70.82	177.94
2b $[NiL'_2(OAc)_2] \rightarrow [NiL'(OAc)_2]$	215–250	–	230	72.80	–	118.05	234.69
2c $[NiL'(OAc)_2] \rightarrow Ni(AcO)_2$	250–315	–	286	128.37	98.47	750.81	1335.96
2d $Ni(AcO)_2 \rightarrow NiCO_3$	315–400	–	382	106.95	–	92.62	141.41
3a $[NiL''_2](AcO)_2\cdot 2H_2O \rightarrow [NiL''_{1.5}](AcO)_2$	50–130	100 [b], 115	–	69.66	87.14	140.73	377.29
3b $[NiL''_{1.5}](AcO)_2 \rightarrow [NiL''(OAc)_2]$	130–170	160	–	135.30	–	30.58	70.62
3c $[NiL''(OAc)_2] \rightarrow [NiL''_{0.5}(OAc)_2]$	170–237	178, 220 [b]	–	102.53	–	18.41	37.34
3d $[NiL''_{0.5}(OAc)_2] \rightarrow Ni(AcO)_2$	237–280	270 [b], 280	–	159.45	–	59.70	109.94
3e $Ni(AcO)_2 \rightarrow NiCO_3$	280–310	–	–	374.85	–	–	–
3f $NiCO_3 \rightarrow NiO$	310–600	–	410	79.25	–	411.93	603.12
4a $[ZnL(OAc)_2]\cdot H_2O \rightarrow [ZnL(OAc)_2]$	40–145	100	–	24.51	43.44	26.22	70.29
4b $[ZnL(OAc)_2] \rightarrow [ZnL_{0.5}(OAc)_2]$	145–170	160	–	319.2	–	78.19	180.58
4c $[ZnL_{0.5}(OAc)_2] \rightarrow Zn(AcO)_2$	170–440	–	343 [b], 392	24.25	–	159.20	258.44

5a $[ZnL'_2(OAc)_2]\cdot 2H_2O \rightarrow [ZnL'(OAc)_2]$	100–190	158	–	78.57	108.87	104.00	241.30
5b $[ZnL'(OAc)_2] \rightarrow Zn(AcO)_2$	190–320	210	304 [b]	80.20	166.57	81.41	141.09
6a $[ZnL''(OAc)_2]\cdot H_2O \rightarrow [ZnL''(OAc)_2]$	30–80	63	–	56.96	74.97	23.83	71.10
6b $[ZnL''(OAc)_2] \rightarrow [ZnL''_{0.5}(OAc)_2]$	80–175	132	–	56.92	89.04	16.60	40.99
6c $[ZnL''_{0.5}(OAc)_2] \rightarrow Zn(AcO)_2$	175–390	–	360	31.77	123.02	55.19	87.19
7a $[CdL(OAc)_2]\cdot H_2O \rightarrow [CdL(OAc)_2]$	50–105	100	–	100.22	197.81	39.51	105.92
7b $[CdL(OAc)_2] \rightarrow Cd(AcO)_2$	150–267	263	–	100.55	231.47	19.83	37.00
7c $Cd(AcO)_2 \rightarrow CdCO_3$	267–300	–	300	292.15	–	–	–
7d $CdCO_3 \rightarrow CdO$	300–440	–	316 [b], 332	439.88	–	114.99	195.23
8a $[CdL'(OAc)_2]\cdot H_2O \rightarrow [CdL'(OAc)_2]$	50–115	110	–	68.29	92.21	31.24	81.57
8b $[CdL'(OAc)_2] \rightarrow [CdL'_{0.5}(OAc)_2]$	115–165	145	–	87.66	93.58	21.54	51.53
8c $[CdL'_{0.5}(OAc)_2] \rightarrow Cd(AcO)_2$	165–320	318	–	41.34	–	57.62	97.50
8d $Cd(AcO)_2 \rightarrow CdCO_3$	320–350	–	345	419.07	–	20.61	33.35
9a $[CdL''(OAc)_2]\cdot 0.5H_2O \rightarrow [CdL''_{0.5}(OAc)_2]$	80–205	175 [b], 192	–	47.53	–	51.94	115.94
9b $[CdL''_{0.5}(OAc)_2] \rightarrow Cd(AcO)_2$	205–290	278	–	71.97	–	–	–
9c $Cd(AcO)_2 \rightarrow CdCO_3$	290–340	–	304	212.75	43.35	162.01	280.78

[a] L = piperazine, L′ = *N*-methylpiperazine, L″ = 1,4-diazacycloheptane (homopiperazine). [b] Temperatures used for the calculation of ΔS.

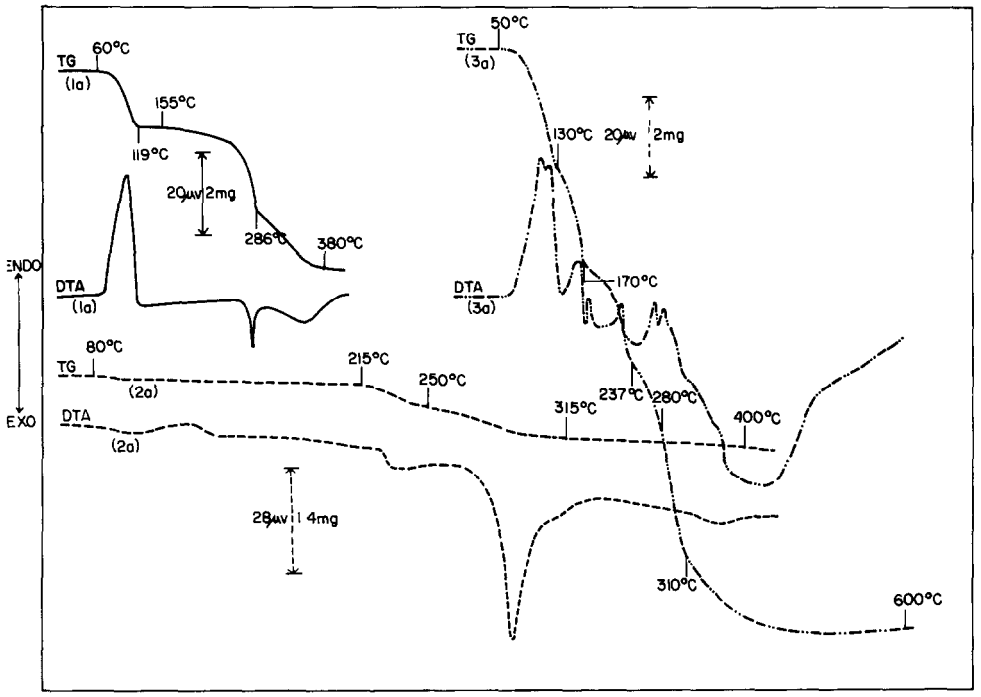

Fig. 1. Thermal curves of $[Ni(pipz)(OAc)_2]\cdot 4H_2O$ (**1a**) (———) (sample mass, 7.58 mg), $[Ni(mpipz)_2(OAc)_2]\cdot 2H_2O$ (**2a**) (- - - - -) (sample mass, 1.76 mg) and $[Ni(dach)_2](AcO)_2\cdot 2H_2O$ (**3a**) (- · · · -) (sample mass, 18.60 mg).

respectively. ΔH can be evaluated from the DTA curves using the relation [22] $\Delta H = KA$, where K is the heat transfer coefficient (cell constant; here the cell is a platinum crucible) and A is the total area under the particular DTA curve. ΔS can be calculated from the relation, $\Delta S = \Delta H/T_m$, where T_m is the DTA peak temperature in kelvin [23]. Values of ΔH for the steps 1(a), 1(b) and 1(c) are 190.22, 29.28 and 60.01 kJ mol^{-1}, respectively, while those of ΔS are 501.90, 61.64 and 95.41 J K^{-1} mol^{-1}, respectively.

The blue colour and the value of the magnetic moment ($\mu_{eff} = 3.26$ BM) of complex **1a** show that it has an octahedral configuration (Scheme 1). In this complex, the pipz ligand functions as a bidentate chelating agent in the boat form. This is shown by the appearance of a larger number of IR spectral bands between 700 and 1400 cm^{-1} (Table 2) than those observed for the free ligand, which exists in the chair form [2,6,18]. The acetate ion may function as a bidentate chelating agent, as shown by the separation ($\Delta\nu$) between $\nu_{as}(CO_2^-)$ and $\nu_s(CO_2^-)$ [11,13–15,24] (120 cm^{-1}) (Table 2). The molar conductance of **1a** was not measured because of its insolubility in many organic solvents. The probable path of decomposition of complex **1a** is given in Scheme 1.

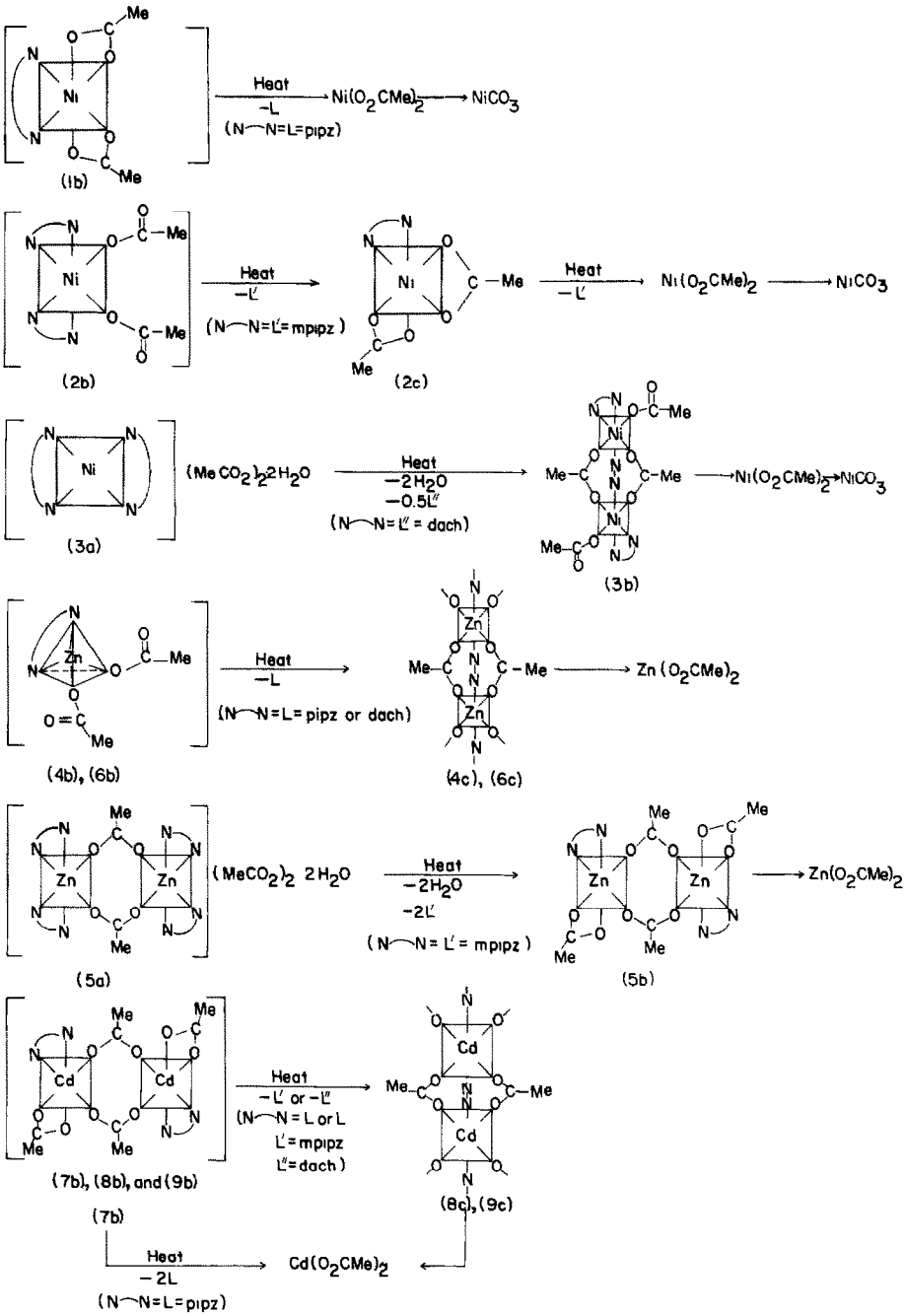

Scheme 1

[Ni(mpipz)$_2$(OAc)$_2$] · 2H$_2$O (2a)

The anhydrous form of this complex has been reported by Marcotrigiano et al. [14]. These workers studied its stereochemistry using IR and electronic

spectroscopies and magnetic moment data; however, no thermal investigation was undertaken. The presence of lattice water in the complex is confirmed by IR spectral data and thermal data (Tables 2 and 3). On heating, the complex first undergoes dehydration in the range 80–215 °C (TG curve). The corresponding DTA curve shows an endothermic peak at 125 °C (Fig. 1). The anhydrous complex $[Ni(mpipz)_2(OAc)_2]$ (**2b**) is converted into $NiCO_3$ via the formation of intermediates $[Ni(mpipz)(OAc)_2]$ (**2c**) and $Ni(AcO)_2$. This process occurs in three steps, 2(b), 2(c) and 2(d), in the ranges 215–250, 250–315 and 315–400 °C, respectively (Fig. 1 and Table 3). Values of E_a^* for the conversions **2a** → **2b**, **2b** → **2c**, **2c** → $Ni(AcO)_2$ and $Ni(AcO)_2$ → $NiCO_3$ are shown in Table 3, which also shows the values of ΔH and ΔS for these conversions.

As indicated by its colour, magnetic moment ($\mu_{eff} = 3.20$ BM) and composition, complex **2a** probably has an octahedral configuration.

In complex **2a**, the ligand mpipz acts as a bidentate chelating agent (boat form) as indicated by IR spectral data (Table 2). This is the same as in complex **1a**. The acetate ion in complex **2a** may function as a unidentate ligand as shown by the value of $\Delta\nu$ (Table 2) (180 cm^{-1}) [11]. The probable path of decomposition of complex **2a** is shown in Scheme 1.

$[Ni(dach)_2](AcO)_2 \cdot 2H_2O$ (3a)

This complex has not been reported previously. It is yellow, diamagnetic and may have a square planar configuration [1]. As in the case of the dach complex reported previously [3], a purple complex (expected to be a tris-complex) is observed in solution on treating the filtrate obtained from the separation of the yellow complex **3a** with an excess of the dach ligand, or on treating a little of the nickel acetate in dry ethanol with an excess of the ligand. This complex was not isolated. The presence of lattice water in **3a** is confirmed as in complex **1a**. On heating, complex **3a** first undergoes dehydration with the loss of one-half of the ligand (dach) in the temperature range 50–130 °C (Fig. 1) to form the complex $[Ni(dach)_{1.5}](AcO)_2$ (**3b**). Complex **3b** is converted into NiO via the formation of intermediates, $[Ni(dach)(OAc)_2]$ (**3c**), $[Ni(dach)_{0.5}(OAc)_2]$ (**3d**), $Ni(AcO)_2$ and $NiCO_3$ in the temperature ranges given in Table 3.

In complex **3a**, the dach ligand acts as a bidentate chelating agent, while the acetate ions may exist as free ions as indicated by the IR spectral data [9] ($\Delta\nu = 140(150)$ cm^{-1}). This supports the square planar structure of **3a**, although the value of the molar conductance for **3a** ($\Lambda_m = 9.0$ ohm^{-1} cm^2 mol^{-1} at 24 °C) is very low for the bi-univalent system [25]. The probable path of decomposition of **3a** is shown in Scheme 1.

$[Zn(pipz)(OAc)_2] \cdot H_2O$ (4a) and $[Zn(dach)(OAc)_2] \cdot H_2O$ (6a)

These complexes have not been reported previously. On pyrolysis, both complexes first undergo dehydration in the range given in Table 3 to form

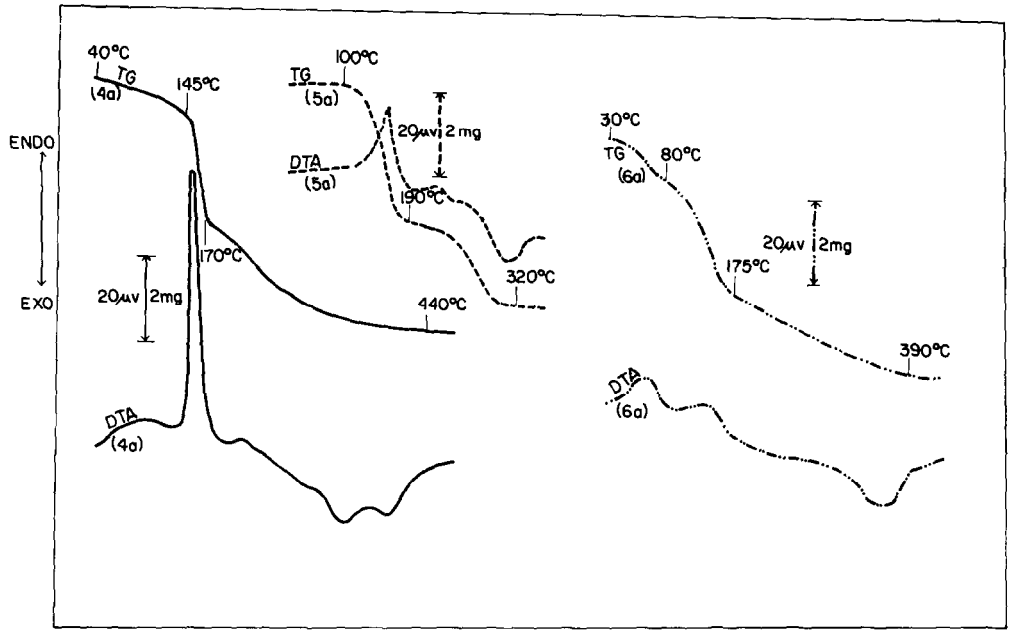

Fig. 2. Thermal curves of $[Zn(pipz)(OAc)_2]\cdot H_2O$ (**4a**) (———) (sample mass, 15.80 mg), $[Zn(mpipz)_2(OAc)_2]\cdot 2H_2O$ (**5a**) (- - - -) (sample mass, 8.72 mg) and $[Zn(dach)(OAc)_2]\cdot H_2O$ (**6a**) (- · · · -) (sample mass, 18.23 mg).

the anhydrous complexes $[Zn(pipz)(OAc)_2]$ (**4b**) and $[Zn(dach)(OAc)_2]$ (**6b**). These cannot be isolated because of their instability (Fig. 2). Complexes **4b** and **6b** decompose to their corresponding acetates in two steps via the intermediates $[Zn(pipz)_{0.5}(OAc)_2]$ (**4c**) and $[Zn(dach)_{0.5}(OAc)_2]$ (**6c**) (Table 3).

In **4a** and **6a**, the ligands (pipz and dach) act as bidentate chelating agents, while the acetate ion functions as a unidentate ligand as supported by IR data [11] ($\Delta\nu = 180$ cm^{-1} for **4a** and 175 cm^{-1} for **6a**) (Table 2). Furthermore, they are non-electrolytes (Λ_m for **4a** at 27 °C = 3.65 ohm^{-1} cm^2 mol^{-1} and Λ_m for **6a** at 27 °C = 5.41 ohm^{-1} cm^2 mol^{-1}) and therefore probably have a tetrahedral configuration (complexes of Zn(II) usually possess this type of configuration [26]). However, **4c** and **6c** may have a polymeric structure (Scheme 1) in which zinc(II) has a coordination number of six and the cyclic ligand (pipz or dach) and acetate ions function as bridging bidentate agents. The paths of decomposition are shown in Scheme 1.

$[Zn(mpipz)_2(OAc)_2]\cdot 2H_2O$ (5a)

This complex has not been reported previously. It is white in colour and its lattice water is confirmed by IR data and thermal curves (Fig. 2). The

complex is converted into $Zn(AcO)_2$ under non-isothermal conditions via the formation of an intermediate $[Zn(mpipz)(OAc)_2]$ (**5b**). This process occurs in two steps, 5(a) and 5(b), in the ranges 100–190 and 190–320 °C, respectively (Table 3 and Fig. 2).

In complex **5a**, the ligand mpipz exists in the boat form as shown by IR data [2] (Table 2) and functions as a bidentate chelating agent. As complex **5a** behaves as a non-electrolyte ($\Lambda_m = 3.3$ ohm^{-1} cm^2 mol^{-1} at 25 °C), acetate ions probably remain inside the coordination sphere and act as unidentate ligands, although the $\Delta\nu$ value is slightly lower than that required for unidentate character. Therefore complex **5a** probably has an octahedral configuration [26]. The probable path of decomposition of **5a** is given in Scheme 1.

*$[Cd(pipz)(OAc)_2] \cdot H_2O$ (**7a**), $[Cd(mpipz)(OAc)_2] \cdot H_2O$ (**8a**) and $[Cd(dach)(OAc)_2] \cdot 0.5H_2O$ (**9a**)*

These complexes have not been reported previously. They are white and appear to be non-electrolytes (Λ_m values for **7a** at 24 °C and for **8a** and **9a** at 27 °C are 5.45, 1.79 and 4.04 ohm^{-1} cm^2 mol^{-1}, respectively). The presence of lattice water is confirmed as in complex **1a**. Under non-isother-

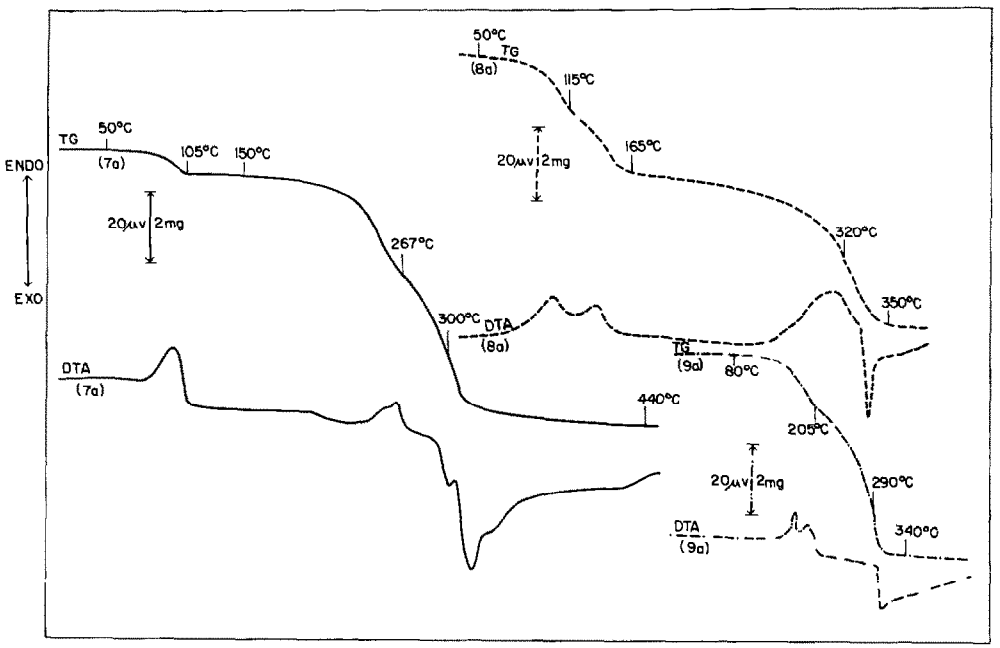

Fig. 3. Thermal curves of $[Cd(pipz)(OAc)_2] \cdot H_2O$ (**7a**) (———) (sample mass, 12.20 mg), $[Cd(mpipz)(OAc)_2] \cdot H_2O$ (**8a**) (- - - - - -) (sample mass, 16.88 mg) and $[Cd(dach)(OAc)_2] \cdot 0.5H_2O$ (**9a**) (- · · · · -) (sample mass, 9.42 mg).

mal conditions complexes **7a** and **8a** first undergo dehydration in the ranges 50–105 and 50–115 °C, respectively, while complex **9a** is converted into $[Cd(dach)_{0.5}(OAc)_2]$ (**9b**) in the range 80–205 °C (Fig. 3). The anhydrous complex $[Cd(pipz)(OAc)_2]$ (**7b**) transforms into CdO in three steps via intermediates $Cd(AcO)_2$ and $CdCO_3$ (Table 3). The complex $[Cd(mpipz)(OAc)_2]$ (**8b**) is converted into $CdCO_3$ in three steps via the intermediates $[Cd(mpipz)_{0.5}(OAc)_2]$ (**8c**) and $Cd(AcO)_2$ in the ranges given in Table 3. Complex **9b** decomposes into $CdCO_3$ in two steps, 9(b) and 9(c), in the ranges 205–290 and 290–340 °C, respectively (Table 3).

As indicated by the IR data ($\Delta\nu$: **7a**, 145 cm^{-1}; **8a**, 130 cm^{-1}; **9a**, 140 cm^{-1}) and the non-electrolytic nature of these complexes, acetate ions function as chelating and bridging bidentate agents, while the cyclic ligands function as bidentate chelating agents. Therefore all the complexes probably have an octahedral structure (cadmium(II) complexes usually possess this type of structure [26]). Furthermore, the broad nature of the $\nu_{as}(CO_2^-)$ bands (Table 2) of these complexes also suggests the presence of more than one type of acetato group [17]. The probable paths of decomposition of **7a**, **8a** and **9a** are shown in Scheme 1.

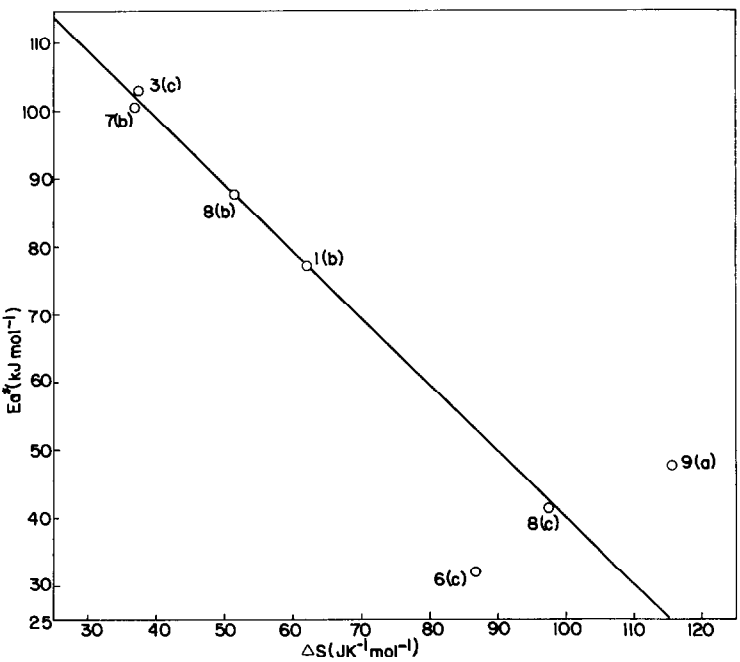

Fig. 4. Plots of E_a^* vs. ΔS values for the conversions: $[Ni(pipz)(OAc)_2] \rightarrow Ni(AcO)_2$, 1(b); $[Ni(dach)(OAc)_2] \rightarrow [Ni(dach)_{0.5}(OAc)_2]$, 3(c); $[Zn(dach)_{0.5}(OAc)_2] \rightarrow Zn(AcO)_2$, 6(c); $[Cd(pipz)(OAc)_2] \rightarrow Cd(AcO)_2$, 7(b); $[Cd(mpipz)(OAc)_2] \rightarrow [Cd(mpipz)_{0.5}(OAc)_2]$, 8(b); $[Cd(mpipz)_{0.5}(OAc)_2] \rightarrow Cd(AcO)_2$, 8(c); $[Cd(dach)(OAc)_2] \cdot 0.5H_2O \rightarrow [Cd(dach)_{0.5}(OAc)_2]$, 9(a).

From the activation energies E_a^* of the initial decomposition steps, the order of stability of the complexes follows the trend pipz > mpipz > dach (Table 3). The *N*-alkylation of the mpipz ligand should increase the stability of the mpipz complexes due to the increased basicity. However, the steric effect causes decreased stability [27,28]. Furthermore, the increase in the ring size of the ligand on introduction of a methylene group between the amine functions causes the decreased stability of the dach complexes, although the strain in the ligand may be reduced.

A linear correlation is obtained on plotting E_a^* vs. ΔS. This shows that a system with a higher entropy change ΔS will require less energy E_a^* for its thermal decomposition [3,4,23] (Fig. 4).

ACKNOWLEDGEMENTS

The authors wish to thank the Government of Manipur, Manipur, India for granting one of them (L.K. Singh) study leave under the F.I.P. scheme. They are also very grateful to Professor N. Ray Chaudhuri, Indian Association for the Cultivation of Science, Calcutta 32, India for his valuable help and encouragement and to C.D.R.I., Lucknow, India, for elemental analyses.

REFERENCES

1 W.K. Musker and M.S. Hussain, Inorg. Chem., 8 (1969) 528.
2 P.J. Hendra and D.B. Powell, J. Chem. Soc., (1960) 5105.
3 L.K. Singh and S. Mitra, J. Chem. Soc., Dalton Trans., (1987) 2089.
4 L.K. Singh and S. Mitra, Inorg. Chim. Acta, 133 (1987) 141.
5 R.A. Walton, J. Chem. Soc. A, (1967) 1852.
6 G.W.A. Fowles, D.A. Rice and R.A. Walton, J. Chem. Soc. A, (1968) 1842.
7 G.W.A. Fowles, D.A. Rice and R.A. Walton, J. Inorg. Nucl. Chem., 31 (1969) 3119.
8 G.W.A. Fowles, D.A. Rice and R.A. Walton, Spectrochim. Acta, Part A, 26 (1970) 143.
9 K. Nakamoto, Infrared and Raman Spectra of Inorganic and Coordination Compounds, 3rd edn., Wiley-Interscience, New York, 1978, p. 232 and references cited therein.
10 R.C. Mehrotra and R. Bohra, Metal Carboxylates, Academic Press, London, 1983, pp. 48, 122 and 129.
11 N.F. Curtis, J. Chem. Soc. A, (1968) 1579.
12 D.F. Steele and T.A. Stephenson, J. Chem. Soc., Dalton Trans., (1972) 2161.
13 S.D. Robinson and M.F. Uttley, J. Chem. Soc., Dalton Trans., (1973) 1912.
14 G. Marcotrigiano, G.C. Pellacani and C. Preti, Z. Anorg. Allg. Chem., 408 (1974) 313.
15 N.W. Alcock and V.M. Tracy, J. Chem. Soc., Dalton Trans., (1976) 2243.
16 B.S. Manhas, A.K. Trikha and M. Singh, Indian J. Chem. Sect. A, 20 (1981) 196.
17 R. Kapoor, R. Sharma and P. Kapoor, Indian J. Chem. Sect. A, 24 (1985) 761.
18 F.G. Mann and H.R. Watson, J. Chem. Soc., (1958) 2772.
19 A.I. Vogel, A. Textbook of Practical Organic Chemistry, 4th edn., ELBS and Longmans, London, 1980, pp. 269, 272.
20 A.I. Vogel, A Textbook of Quantitative Inorganic Analysis, 3rd edn., ELBS and Longmans, London, 1968, pp. 389, 390, 480.

21 H.H. Horowitz and G. Metzger, Anal. Chem., 35 (1963) 1464.
22 H.J. Borchardt and F. Daniels, J. Am. Chem. Soc., 79 (1957) 41.
23 R. Roy, M. Chaudhury, S.K. Mandal and K. Nag, J. Chem. Soc., Dalton Trans., (1984) 1681.
24 C. Rocchioccioli-Deltcheff, R. Franck, V. Cabuil and R. Massart, J. Chem. Res. (S), (1987) 126.
25 P.R. Shukla, B.B. Awasthi and R. Rastogi, Indian J. Chem., 23A (1984) 241.
26 F.A. Cotton and G. Wilkinson, Advanced Inorganic Chemistry, 3rd edn., Wiley-Interscience, New York, 1972, pp. 504, 505.
27 W.K. Musker and M.S. Hussain, Inorg. Chem., 5 (1966) 1416.
28 J.E. Huheey, Inorganic Chemistry, 3rd edn., Harper International, New York, 1983, pp. 298, 299.